Thermal decomposition of metazeunerite- a high resolution thermogravimetric and hot-stage Raman spectroscopic study

Ray L. Frost•, Matt L. Weier and Moses O. Adebajo

Inorganic Materials Research Program, School of Physical and Chemical Sciences, Queensland University of Technology, GPO Box 2434, Brisbane Queensland 4001, Australia.

Published as:
R.L. Frost, M.L. Weier, and M.O. Adebajo, Thermal decomposition of metazeunerite-a high-resolution thermogravimetric and hot-stage Raman spectroscopic study. Thermochimica Acta, 2004. 419(1-2): p. 119-129

Abstract

A combination of high resolution thermogravimetric analysis coupled to a gas evolution mass spectrometer has been used to study the thermal decomposition of metazeunerite $\{Cu(H_2O)_4\}(H_2O)_4[(UO_2)(AsO_4)]_2$. Five stages of weight loss are observed at 48, 88, 125, 882 and 913 °C. In the first three stages 2, 4 and 2 moles of water are lost. In stages 4 and 5 some As_2O_5 units are lost and it is probable that reduction of the anhydrous phase $Cu[(UO_2)(AsO_4)]_2$ occurs. The stages of dehydration were confirmed by the use of evolved water vapour mass spectroscopy. Changes in the structure of metazeunerite were followed by the use of Raman microscopy in conjunction with a thermal stage. Two Raman bands are observed at 818 and 811 cm^{-1} and are assigned to the ν_1 symmetric stretching modes of the UO_2 units. The UO_2 Raman antisymmetric stretching mode was observed at 890 cm^{-1}. No AsO_4 stretching vibrations were observed until after two stages of dehydration of the metazeunerite. The AsO_4 ν_4 bending modes show complexity with bands observed at 463, 446, 396 and 380 cm^{-1}. Thermal treatment results in the removal of this degeneracy. The ν_2 band of the AsO_4 units is observed at 320 cm^{-1}. Raman bands at 275 and 235 cm^{-1} are attributed to the ν_2 bending modes of the $(UO_2)^{2+}$ units. The use of the hot stage Raman microscope enables low temperature phase changes brought about through dehydration to be studied.

Keywords: autunite, meta-autunites, metazeunerite, dehydration, dehydroxylation, Raman spectroscopy, high-resolution thermogravimetric analysis

1. Introduction

There are more than 200 uranium minerals; many of which exist in Australian deposits [1]. The chemistry of uranium is important for the solution of environmental problems; for example the remediation of contaminated sites and the restoration of soils such as might be found at Woomera, Australia [2, 3]. Uranyl phosphates and arsenates form one of the largest and most widespread group of uranium minerals [4].

• Author to whom correspondence should be addressed (r.frost@qut.edu.au)

The minerals are known as autunites and also as the uranyl micas. Many of these minerals may be found in quite widespread parts of Australia [5]. The autunite group of minerals are uranyl arsenates and phosphates with symmetries ranging from tetragonal to triclinic. The minerals have a general formula $M(UO_2)_2(XO_4)_2.8\text{-}12H_2O$ where M may be Ba, Ca, Cu, Fe^{2+}, Mg, Mn^{2+} or ½(HAl) and X is As, or P. Autunites are common minerals, yet have been rarely studied in terms of thermal analysis [6-9] and certainly not in terms of Raman spectroscopy. The minerals have a layer-like structure [8, 10, 11]. The cations and water are located in the interlayer space. The mineral autunite has the formula $Ca[(UO_2)_2(PO_4)]_2.11(H_2O)$. The structure of a synthetic autunite has been solved [10]. Autunite is orthorhombic [10] and saléeite is monoclinic [12, 13]. The structure contains the well-known autunite type sheet with composition $[(UO_2)(PO_4)]$, resulting from the sharing of equatorial vertices of the uranyl square bipyramids with the phosphate or arsenate tetrahedra [14]. The calcium atom in the interlayer is coordinated by seven H_2O groups and two longer distances to uranyl apical O atoms. Two independent H_2O groups are held in the structure only by hydrogen bonding [10].

Most uranyl minerals are hydrated and as such water plays a significant role in their structures. It is common for water to play a major role in the degree of polymerisation because of the asymmetric nature of hydrogen bonding systems. Water may bond to the interstitial cation or may simply be held in the structure through hydrogen bonding. Water groups play an important role in satisfying bond-valence requirements. The role of water and the number of water units in the empirical formula determines structural arrangements in the uranyl mica interlayer [4]. For example:

$Ca(UO_2)_2(PO_4)_2.11H_2O$ (autunite) $\rightarrow Ca(UO_2)_2(PO_4)_2.8H_2O$ (metaautunite)

$Ca(UO_2)_2(PO_4)_2.8H_2O$ (metaautunite) $\rightarrow Ca(UO_2)_2(PO_4)_2.xH_2O$ (partially dehydrated metaautunite).

Burns et al.(1996) proposed that uranyl mineral structures be based upon a topological arrangement of anions within each sheet as a convenient basis for the classification of these sheets [15]. The difference between the autunite group and meta-autunite is simply the number of water molecules in the formula. One major difference between the autunite and metautunite groups is their water content. The moles of water in different autunite species may differ and as a group range from 10 to 12 moles. On the other hand the moles of water in the metaautunite group ranges from 6 to 8 moles. The structure and hydration state of metaautunite have not been satisfactorily determined. Zeunerite is the mineral $\{Cu(H_2O)_4\}(H_2O)_8[(UO_2)(AsO_4)]_2$ and metazeunerite is the mineral $\{Cu(H_2O)_4\}(H_2O)_4[(UO_2)(AsO_4)]_2$ [16, 17].

The use of infrared spectroscopy to study the chemical reactions as illustrated in the above thermal stages of dehydration is difficult in the lower temperature ranges. However Raman spectroscopy combined with a hot stage lends itself as the technique of choice for studying the chemical reactions during dehydration. The structures of copper based synthetic autunites, namely torbernite, metatorbernite, zeunerite and metazeunerite have been solved [16]. Zeunerite and metazeunerite are isostructural with torbernite and metatorbernite [16]. These minerals contain the autunite-type sheet, of composition $[(UO_2)(AsO_4)]^-$ or $[(UO_2)(PO_4)]^-$, which involves the sharing of equatorial vertices of uranyl square bipyramids with phosphate (or arsenate)

tetrahedra. According to Locock and Burns, there is a symmetrically independent H_2O group held in each structure by hydrogen bonding, which in zeunerite forms square planar sets of interstitial water groups both above and below the planes of the Cu^{2+} atoms [16]. In the metazeunerite structure the sets of interstitial water are either above or below the planes of the Cu^{2+} cations. Upon dehydration of the zeunerite to meta-zeunerite, not only is there a loss of 4 moles of water but the space groups change and the orientations of the uranyl arsenate sheets change . Our interest in minerals with clay-like structures causes our motivation in this research as does the search for fundamental knowledge of minerals containing copper and arsenate anions [2, 3, 18, 19]. In this work we report the thermal transformation of metazeunerite, a copper based uranyl arsenate using a combination of high resolution thermogravimetry coupled to an evolved gas mass spectrometer and hot stage Raman microscopy.

2. Experimental

2.1 Minerals

Metazeunerite (M20948), was obtained from Museum Victoria and originated from Gilgai, New England, NSW. The mineral was analysed by X-ray diffraction for phase purity and by electron probe using energy dispersive techniques for quantitative chemical composition.

2.2 X-ray diffraction

` X-Ray diffraction patterns were collected using a Philips X'pert wide angle X-Ray diffractometer, operating in step scan mode, with Cu K_α radiation (1.54052 Å). Patterns were collected in the range 3 to 90 °2θ with a step size of 0.02° and a rate of 30s per step. Samples were prepared as a randomly orientated powder on a petroleum jelly coated glass slide. Data collection and evaluation were performed with PC-APD 3.6 software. Profile fitting was applied to extract information on the microstructure and structural defects of kaolinite and its alteration products. The Profile Fitting option of the software uses a model that employs twelve intrinsic parameters to describe the profile, the instrumental aberration and wavelength dependent contributions to the profile.

2.3 Thermal Analysis

Thermal decomposition of the hydrotalcite was carried out in a TA® Instruments incorporated high-resolution thermogravimetric analyzer (series Q500) in a flowing nitrogen atmosphere (80 cm^3/min). Approximately 50mg of sample was heated in an open platinum crucible at a rate of 2.0 °C/min up to 500°C. With the quasi-isothermal, quasi-isobaric heating program of the instrument the furnace temperature was regulated precisely to provide a uniform rate of decomposition in the main decomposition stage. The TGA instrument was coupled to a Balzers (Pfeiffer) mass spectrometer for gas analysis. Only water vapour, carbon dioxide and oxygen were analyzed.

2.4 Hot Stage Raman microprobe spectroscopy

The crystals of metazeunerite were placed and oriented on the stage of an Olympus BHSM microscope, equipped with 10x and 50x objectives and part of a Renishaw 1000 Raman microscope system, which also includes a monochromator, a filter system and a Charge Coupled Device (CCD). Raman spectra were excited by a HeNe laser (633 nm) at a resolution of 2 cm^{-1} in the range between 100 and 4000 cm^{-1}. Repeated acquisition using the highest magnification was accumulated to improve the signal to noise ratio. Spectra were calibrated using the 520.5 cm^{-1} line of a silicon wafer. In order to ensure that the correct spectra are obtained, the incident excitation radiation was scrambled. Previous studies by the authors provide more details of the experimental technique [3, 20-22]. Spectra at elevated temperatures were obtained using a Linkam thermal stage (Scientific Instruments Ltd, Waterfield, Surrey, England). Details of the technique have been published by the authors [2, 18, 19, 23-25]. Spectral manipulation such as baseline adjustment, smoothing and normalisation was performed using the GRAMS® software package (Galactic Industries Corporation, Salem, NH, USA).

3. Results and discussion

3.1 X-ray diffraction of metazeunerite

The analysis of the sample labelled as Metazeunerite (M20948) from Museum Victoria is shown in Table 1 and compared with the XRD data obtained from JCPDS data base. A study of the data in the table appears to show that the mineral is a mixture of zeunerite and metazeunerite. The d(001) spacing of 10.35 Å for the mineral used in this research corresponds with the 10.3 Å of zeunerite. The d spacing of 8.68 Å corresponds to that of 8.63 Å for metazeunerite.

3.2 High Resolution Thermogravimetric Analysis and Mass spectrometric analysis

The high resolution thermogravimetric analysis of metazeunerite is shown in Figures 1a and 1b. Four steps are involved with the loss of water and two with the loss or reduction of arsenate anions. The first step occurs at 48°C, the second at 88°C, the third at 138 °C and the last step involving water at 255 °C. This last step appears as a broad continuum over an extended temperature range from around 150 °C to 250 °C. The weight loss steps are 3.45%, 7.05 %, 0.87 % and 3.46 % respectively. The total weight loss is 14.83 %. The theoretical weight loss for $Cu(UO_2)_2(AsO_4)_2.8H_2O$ is 14.05 %. The difference between the experimental and theoretical mass losses may be accounted for by adsorbed water. Whilst no low temperature (<40 °C) mass loss is observed in the HRTG experiment, a low temperature water vapour evolution is observed in the MS pattern. This may be attributed to the loss of adsorbed water. This means that the number of moles of water lost in the first step is 2, in the second step 4 and in the third and fourth steps 2 moles. The loss of arsenate occurs over two steps at 882 °C and 913 °C (Figure 1b). The mass loss steps are 8.3 and 4.1 %. The theoretical weight loss for arsenate is 27.0 %. This means that about 50% of the AsO_4 units are lost at 882 and 913 °C. The upper temperature limits of the HRTG are 1000 °C and it is thought that the remainder of the AsO_4 units may be accounted for by

reduction of the U, As and even Cu at the higher temperatures. The mass spectrum of water is shown in Figure 2. This figure shows the MS=18 curve and the DTG curve. The two curves have the same patterns precisely. The figure shows that evolved water vapour mass as the metazeunerite is thermally decomposed. The temperatures of the mass gain are 47, 88.6, 136 and 257 °C. These temperatures match the temperatures of the mass loss steps with absolute precision. The MS of water shows an additional evolved mass gain at 28.7 °C which was not observed in the HRTG patterns and is ascribed to adsorbed water.

Stages of the thermal decomposition of metazeunerite:

Meta-zeunerite may be written as $\{Cu(H_2O)_4\}(H_2O)_4[(UO_2)(AsO_4)]_2$ [16]. The units in the square bracket represent the uranyl arsenate sheet and the remaining part of the formula the interlayer contents. Writing the formula of metazeunerite as such shows the hydration of the Cu^{2+} and the additional water molecules held in place in the interlayer by hydrogen bonding. In the structure of meta-zeunerite the Cu^{2+} is coordinated by four water molecules and by two longer bonds to the apical oxygen atoms of the uranyl ions. Uranyl micas are layered structures with water playing a dominant role in their structures. In this case, the hydrated cations fit between the uranyl arsenate layers [17]. In the case of metazeunerite the uranyl arsenate surface may be considered to be multiple units of $(UO_2.AsO_4)_n$ and functions like a polymeric anion. The anion is counterbalanced by the hydrated copper(II) cation in the interlayer. Dehydration of metazeunerite results in the loss of water from (a) firstly from the interlayer and secondly from around the copper(II) ion is steps..

The mechanism for the dehydration of meta-zeunerite is as follows:

Stage 1

$$\{Cu(H_2O)_4\}(H_2O)_4[(UO_2)(AsO_4)]_2 \rightarrow \{Cu(H_2O)_4\}(H_2O)_2[(UO_2)(AsO_4)]_2 + 2\ H_2O \quad (48\ °C)$$

Stage 2

$$\{Cu(H_2O)_4\}(H_2O)_2[(UO_2)(AsO_4)]_2 \rightarrow \{Cu(H_2O)_2\}[(UO_2)(AsO_4)]_2 + 4\ H_2O \quad (88\ °C)$$

Stage 3

$$\{Cu(H_2O)_2\}[(UO_2)(AsO_4)]_2 \rightarrow Cu[(UO_2)(AsO_4)]_2 + 2\ H_2O \quad (125\ \text{to}\ 250\ °C)$$

Stages 4 & 5

$$Cu(UO_2)_2(AsO_4)_2 \rightarrow CuO(UO_2)_2(AsO_4) + 1/2As_2O_5 \quad (882\ \text{and}\ 913\ °C)$$

The thermal decomposition of metazeunerite may be considered as occurring in a sequence of stages. In Stage 1 at 48 °C, two moles of water are lost. In stage 2, 4 moles of water are lost and in stage 3 a further two moles of water are lost. Thus in three successive stages all 8 moles of water are lost resulting in an anhydrous compound $(Cu(UO_2)_2(AsO_4)_2)$. It is not known whether this chemical retains its layered structure or forms a three dimensional structure with Cu linking the uranyl arsenate groups. The two higher temperature stages are attributed to the loss of arsenate as As_2O_5. In these steps it is not certain whether all the As is lost or that some

is retained to higher temperatures in some reduced form. The upper temperature limit of the HRTG is 1000 °C and any weight losses above this temperature are not determined. It is probable that not all the arsenate is lost at 882 and 913 °C even though the experimental weight loss does not match the theoretical weight loss. It may be possible that the As_2O_5 is condensing in the capillary before reaching the mass spectrometer.

Burns has shown that the U^{6+} cation is almost always present in crystal structures as part of a nearly linear $(UO_2)^{2+}$ uranyl ion that is coordinated by four, five or six equatorial anions in an approximate planar arrangement perpendicular to the uranyl ion, giving square, pentagonal and hexagonal bipyramids [26]. The crystal structure of metazeunerite has been undertaken [27]. Hanic reported that the sheets $[(UO_2)(AsO_4)]$ are separated by layers containing the cations $(Cu(H_2O)_4)^{2+}$ and several moles of H_2O [27]. However this structure presented by Hanic is clearly incorrect [16]. The infrared spectrum of the hydroxyl stretching region of water of metazeunerite shows two intense bands at 3280 and 2923 cm^{-1} with a band of much lower intensity at 3407 cm^{-1}. Bands in these positions are indicative of strongly hydrogen bonded water. One possible model is based upon the water molecules coordinating the copper cation and at the same time hydrogen bonding to the AsO_4 units. The infrared spectrum of the HOH bending region of water in metazeunerite is shown in Figure 3. Only a single HOH deformation band is observed at 1648 cm^{-1}. The reason for the tail on the lower wavenumber side of the spectrum may be attributed to δMOH bands [4]. The observation of a band in this position is an indication that no free water is present [28]. All of the water is in a structured state either in the interlayer or in the hydration sphere of the copper(II) cation.

3.3 Hot Stage Raman spectroscopy of Metazeunerite

Raman spectroscopy of the hydroxyl stretching region using the thermal stage

The Raman spectra of the water OH stretching region of metazeunerite for selected temperatures are shown in Figure 4. It should be noted that the intensity of the hydroxyl stretching region of metazeunerite is low and the hydroxyl stretching region occurs on a steeply sloping background making the determination of the spectra difficult. In the spectrum at 40 °C, four hydroxyl stretching bands are observed at 3748, 3537, 3394 and 3093 cm^{-1}. The bandwidths are 218, 97, 359 and 268 cm^{-1}. In the structure of meta-zeunerite there are two symmetrically independent water positions at room temperature leading to four water groups around the Cu^{2+} and four interstitial water groups. The observation of four OH stretching vibrations suggests that there are four independent water molecules in the metazeunerite structure. Locock and Burns pointed out that in the crystal structure there are two free independent water molecules [16]. The high wavenumber band at 3748 cm^{-1} may be ascribed to this weakly hydrogen bonded water. Hydrogen bonds link these water molecules into the square planar sets of water molecules. The water molecules which coordinate the Cu^{2+} account for the bands observed at 3537, 3394 and 3093 cm^{-1}. In the first stage of thermal decomposition two water molecules are lost at 48 °C. The Raman spectrum at 60 °C shows three OH stretching vibrations at 3436, 2953 and 2811 cm^{-1}. The position of these OH stretching vibrations suggests that partial dehydration in the first stage caused stronger hydrogen bonding in the metazeunerite structure. Further heating above 80 °C results in the loss of four molecules of water

per formula unit. In the Raman spectrum of metazeunerite at 100 °C, four bands are observed at 3681, 3493, 3047 and 2893 cm^{-1}.

Raman spectroscopy shows changes in the structure of metazeunerite upon thermal treatment. The results from Raman spectroscopy support the concept that water is coming off in stages. Previous studies have suggested that the water is lost in a zeolite dehydration behaviour [29]. In such a situation the water escapes through holes in a coherent three-dimensional framework. Such a process is reversible such that upon cooling the water would refill the spaces in the zeolite type structure. The variable hydration state of zeolite type materials is not consistent with the dehydration behaviour of metazeunerite. In contrast to porous materials the water molecules are required to maintain the structural integrity. In this work both the HRTG and the hot-stage Raman spectroscopy shows that the dehydration takes place as a series of steps. The question of reversibility of these hydration steps remains to be proven. The transition of zeunerite to metazeunerite may not be reversible. The reaction is as follows:

$$Cu(UO_2)_2(AsO_4)_2.12H_2O \rightarrow Cu(UO_2)_2(AsO_4)_2.8H_2O + 4H_2O$$

Such a reaction involves the removal of one layer of water either above or below the Cu^{2+} layer. Such a reaction involves the sideways displacement of this Cu^{2+} layer relative to the uranyl arsenate layer. Such displacement is likely to mean that the zeunerite to metazeunerite transition is non-reversible. Other researchers have investigated the dehydration behaviour of autunites, meta-autunite and other uranyl micas and found that the water content in existing phases is constant and does not vary as with zeolites [30, 31]. Dehydration was found to proceed in a stepwise fashion [30, 31]. Such structural arguments agree with the propositions propounded in this study.

3.4 Raman spectroscopy of the UO_2 and AsO_4 stretching region using the thermal stage

Čejka et al. has reported the infrared spectroscopy of many uranyl minerals. [6, 8, 28, 32] The free uranyl ion $(UO_2)^{2+}$ with point symmetry $D_{\infty h}$ should exhibit three fundamental modes symmetric stretching vibration ν_1, bending vibration ν_2 and the antisymmetric stretching vibration ν_3. The bending mode is doubly degenerate since it can occur in two mutually independent planes. [28] Hence the linear uranyl group has four normal vibrations but only three fundamentals. In a linear symmetric uranyl ion belonging to the $D_{\infty h}$ point group the ν_1 band is found in the 900 to 750 cm^{-1} region and is Raman active but only appears in the infrared spectrum in the case of substantial symmetry lowering. The antisymmetric stretching vibration is active in the infrared and inactive in the Raman. Lowering of the symmetry results in the activation of all fundamentals. Farmer reported the infrared spectral results of some autunite minerals. [33] The values for torbernite were listed as ν_1 mode at 915 cm^{-1}, ν_2 as 465 cm^{-1}, ν_3 as 1115 and 1023 cm^{-1} and ν_4 as 615 and 550 cm^{-1}. Farmer gave the position of the $(UO_2)^{2+}$ bands as ν_1 at 805 cm^{-1} for torbernite and ν_3 as 915 cm^{-1}. The interpretation of this assignment is open to question. Čejka et al. reported the infrared spectrum of sabugalite and suggested that the weak absorption band at 810 cm^{-1} was attributable to the symmetric stretching mode of the $(UO_2)^{2+}$ unit and that the band at 915 cm^{-1} was attributable to the antisymmetric stretching vibration of the $(UO_2)^{2+}$ unit.

[6] The ν_2 bands of the $(UO_2)^{2+}$ units were found at 298 and 254 cm^{-1}. Herein lies the difficulty in that both the ν_1 bands of AsO_4 and $(UO_2)^{2+}$ is found at the same spectral positions making interpretation by vibrational spectroscopy difficult.

The Raman spectra of the AsO_4 and UO_2 stretching region as a function of temperature are shown in Figure 5. The results of the band component analyses are reported in Table 2. The symmetric stretching vibration of the aqueous arsenate anion (ν_1) is observed at 810 cm^{-1} and coincides with the asymmetric stretching mode (ν_3). The bending modes (ν_2) and (ν_4) are observed at 342 cm^{-1} and at 398 cm^{-1} respectively. Herein lies a problem in the vibrational spectroscopy of the arsenate containing uranyl micas. The bands associated with the AsO_4 stretching vibrations are coincident with the UO_2 stretching vibrations. A band is observed at 890 cm^{-1} and is sharp with a bandwidth of 10.0 cm^{-1}. This band is assigned in accordance with the attribution of Čejka et al. to the UO_2 ν_3 antisymmetric stretching modes. The band is asymmetric on the high wavenumber side suggesting two overlapping bands. Such a concept fits well with the non-equivalence of the two UO_2 bonds [16]. The band at 890 cm^{-1} shifts to 902 cm^{-1} upon thermal treatment above 50 °C. It is apparent that the loss of two water molecules according to stage 1 in the HRTG results changes the position of the ν_3 antisymmetric stretching vibration. These two water molecules are the two interstitial water molecules in the metazeunerite structure. The bandwidth of the 890/902 cm^{-1} band increases then decreases upon thermal treatment with the maximum bandwidth at 80 °C.

In the 20°C spectrum two bands are observed at 818 and 811 cm^{-1} with bandwidths of 7.5 and 10.8 cm^{-1}. The first band shifts to 822 cm^{-1} at 40 °C. However there is a significant change in the relative intensities of the 818/811 cm^{-1} bands upon heating from 20 to 40 °C. These two bands are assigned in accordance with Čejka et al. as the ν_1 stretching modes of the UO_2 units [28]. It is possible that the change in the band position of the 818 cm^{-1} band is due to an intensity contribution from the symmetric stretching mode of the AsO_4 units. Alternatively the band is an additional band brought about through a stronger bonding of the UO_2 to the Cu^{2+} cations. Dehydration forces the Cu^{2+} to bond to the UO_2 groups. This bonding is observed as increased intensity in the ~854 and 841 cm^{-1} bands. This means that the two UO_2 bands at ~825 and 807 cm^{-1} are associated with non-bonding or weak bonding. In the structure of zeunerite proposed by Locock and Burns the Cu^{2+} is bonded to two uranyl oxygens linearly at long interatomic distances of 2.482 Å. In the structure of metazeunerite the Cu---O_{uranyl} bond distances are 2.445 and 2.645 Å. Dehydration forces the distance between the UO_2 units and the Cu^{2+} to increase slightly. The reason for this slight increase is the shuffling of the uranyl-arsenate layer relative to the Cu^{2+} atoms. This results in the additional band in the UO_2 stretching region.

Upon heating the metazeunerite to 60 °C, the band profile broadens and becomes more complex. The two bands now shift to 813 and 801 cm^{-1} and are attributed to the UO_2 symmetric stretching vibrations. At the same time an additional band at 873 cm^{-1} is observed. This band is assigned to the ν_3 antisymmetric stretching mode of the AsO_4 units. The non-equivalence of the two UO_2 bonds affects the AsO distances and results in the non-equivalence of the AsO_4 bonds. In terms of Raman spectroscopy this means that the AsO_4 symmetric stretching vibration will be either inactive or of low intensity. Alternatively the UO_2 and AsO_4 symmetric stretching

vibrations couple and only one band is observed. Thermal treatment above 80 °C results in the appearance of an additional band at 844 cm^{-1} which is assigned to the ν_1 AsO_4 symmetric stretching vibration. The effect of thermal treatment with dehydration results in the uncoupling of the UO_2 and AsO_4 symmetric stretching vibrations. In the 80 °C spectrum the two UO_2 stretching vibrations are observed at 822 and 807 cm^{-1} and are broad with bandwidths of 46.8 and 24.9 cm^{-1}. Significant changes are observed in the band profile in the 750 to 850 cm^{-1} region upon heating from 80 to 100 °C. These changes are associated with the loss of water in stage 2 of the dehydration steps at 88 °C. The Raman spectra above 50 °C show an additional band at around 775 cm^{-1}. This band is assigned to a water librational mode. The band becomes Raman active after 60 °C and probably results from the hydrogen bonding of water to the AsO_4 units. It is noted that the intensity approaches zero in the 120 °C spectrum.

3.5 Raman spectroscopy of the AsO_4 bending region using the thermal stage

The Raman spectroscopy of the UO_2 and AsO_4 bending region has the advantage that the two bending regions are well separated (Figure 6). The AsO_4 bending region occurs between 300 and 500 cm^{-1} and the UO_2 bending region below 300 cm^{-1}. The bending modes (ν_2) of aqueous AsO_4 occur at 342 cm^{-1}. Thus the sharp band at 320 cm^{-1} for metazeunerite is assigned to the OAsO in plane bending mode. The band at 20 and 40 °C is sharp with bandwidths of 7.1 and 6.6 cm^{-1} respectively. At 60 °C the band is observed at 322 cm^{-1} with an increased bandwidth of 16.7 cm^{-1}. The bending mode (ν_4) of the AsO_4 is observed at 398 cm^{-1} in aqueous systems. In the 20 °C spectrum four bands are observed at 463, 446, 396 and 380 cm^{-1}. The latter two bands are of low intensity. All four bands are quite sharp with bandwidths of 19.0, 20.1, 10.8 and 12.8 cm^{-1} respectively. At 40 °C, three bands are observed at 461, 448 and 398 cm^{-1} with considerably increased bandwidths. At 60 °C and above only a single band is observed at 452 cm^{-1}. The significance of the changes in the spectrum of the ν_4 bending region is the removal of the loss of degeneracy upon thermal treatment. An additional broad band is observed at 376 cm^{-1} and is assigned to a second ν_4 bending mode.

In the very low wavenumber region, three bands are observed in the 298 K spectrum at 275, 235 and 218 cm^{-1}. The bands at 275 and 235 cm^{-1} are attributed to the ν_2 bending modes of the $(UO_2)^{2+}$ units. The band at 218 cm^{-1} is assigned to lattice vibrations. Other bands are observed around 182 and 139 cm^{-1} and are also described as lattice modes.

4. Conclusions

A combination of high resolution thermogravimetric analysis coupled to a gas evolution mass spectrometry has been used to study the thermal decomposition of the mineral meta-zeunerite ($Cu(UO_2)_2(AsO_4)_2.8H_2O$). Five stages of weight loss are observed at 48, 88, 125, 882 and 913 °C. In the first three stages 2, 4 and 2 moles of water are lost. In stages 4 and 5 As_2O_5 units are lost and it is probable that reduction of the As, U and even Cu occurs. The stages of dehydration were confirmed by the use of evolved water vapour mass spectrum. The temperatures of these dehydration steps were then used as the temperatures at which Raman spectra of the thermally

decomposed sample were obtained. These Raman spectra were then used to characterise the changes in the molecular structure of the metazeunerite. Very significant changes in the Raman spectra were obtained at these temperatures. The crystal structure of metazeunerite shows that the structure is a tetragonal structure. This distortion is maintained by the hydrogen bonding of the water molecules to the AsO_4 and UO_2 units which form a layer either above or below the plane of the Cu^{2+} atoms. The loss of water between 40 and 55 °C results in the removal of interstitial water resulting in Raman spectra of increasing complexity. Further dehydration above 100 °C results in the loss of the layer structure, resulting in further increased complexity in the Raman spectra. Dehydration of the mineral is readily followed by the changes in the spectra of the water OH stretching region.

One of the difficulties in assigning the bands of the autunite-metaautunite minerals is the overlap of the stretching vibrations of the UO_2 and AsO_4 and/or PO_4 units. The AsO_4 and UO_2 stretching vibrations occur in almost identical positions. The further complexity is introduced because of the distorted structure of the metazeunerite unit cell. In the structure of metazeunerite the four AsO bonds are non-equivalent brought about by the non-equivalence of the two UO_2 bonds. Such non-equivalence results in the lack of intensity of the ν_1 AsO_4 stretching band. This band only becomes observed after the initial dehydration steps which results in the removal of the layered water structure. No symmetric stretching vibration is observed until after significant dehydration has occurred at 80 °C, when a low intensity band at 827 cm^{-1} is observed. The structure of metazeunerite is such that the two UO bonds are non-equivalent. These results in the observation of two UO stretching bands observed at 818 and 811 cm^{-1}. A low intensity band is observed at around 890 cm^{-1} and is attributed to the UO_2 antisymmetric stretching vibration. A complex set of bands is observed in the low wavenumber region. These bands are assigned to the UO_2 bending vibrations. Bands are observed at 275, 235, 218 and 182 cm^{-1} and are all assigned to UO_2 bending modes. The complexity of the UO_2 bending modes is observed up to 250 °C. This complexity is lost only after dehydration.

5. References

1. I. M. Threadgold, CSIRO Mineragraphic Investigations Technical Paper No. 2. (1960).
2. R. L. Frost, T. Kloprogge, M. L. Weier, W. N. Martens, Z. Ding and H. G. H. Edwards, Spectrochimica Acta, Part A: Molecular and Biomolecular Spectroscopy 59 (2003) 2241.
3. R. L. Frost, M. L. Weier, W. Martens, J. T. Kloprogge and Z. Ding, Thermochimica Acta 403 (2003) 237.
4. P. Burns, Reviews in mineralogy Vol 38 (1999) 23.
5. H. Isobe, R. C. Ewing and T. Murakami, Materials Research Society Symposium Proceedings 333 (1994) 653.
6. J. Cejka, Z. Urbanec, J. Cejka, Jr., J. Ederova and A. Muck, Journal of Thermal Analysis 33 (1988) 395.
7. T. L. Ambartsumyan, Atomnaya Energ., Voprosy Geol. Urana, Suppl. (1957) 86.
8. J. Cejka, J. Cejka, Jr. and A. Muck, Thermochimica Acta 86 (1985) 387.
9. T. Muto, Mineralogical Journal 4 (1965) 245.
10. A. J. Locock and P. C. Burns, American Mineralogist 88 (2003) 240.

11. J. Cejka, Jr., A. Muck and J. Cejka, Physics and Chemistry of Minerals 11 (1984) 172.
12. C. Frondel, American Mineralogist 36 (1951) 680.
13. S. A. Miller and J. C. Taylor, Zeitschrift fuer Kristallographie 177 (1986) 247.
14. J. Beintema, Recueil des Travaux Chimiques des Pays-Bas et de la Belgique 57 (1938) 155.
15. P. C. Burns, M. L. Miller and R. C. Ewing, Canadian Mineralogist 34 (1996) 845.
16. A. J. Locock and P. C. Burns, Canadian Mineralogist 41 (2003) 489.
17. K. Walenta, Chemie der Erde 24 (1965) 254.
18. W. Martens, R. L. Frost and P. A. Williams, Journal of Raman Spectroscopy 34 (2003) 104.
19. W. N. Martens, R. L. Frost, J. T. Kloprogge and P. A. Williams, American Mineralogist 88 (2003) 501.
20. R. L. Frost and M. L. Weier, Thermochimica Acta 406 (2003) 221.
21. R. L. Frost and Z. Ding, Thermochimica Acta 405 (2003) 207.
22. E. Horvath, R. L. Frost, E. Mako, J. Kristof and T. Cseh, Thermochimica Acta 404 (2003) 227.
23. R. L. Frost, M. Crane, P. A. Williams and J. T. Kloprogge, Journal of Raman Spectroscopy 34 (2003) 214.
24. R. L. Frost, Spectrochimica Acta, Part A: Molecular and Biomolecular Spectroscopy 59A (2003) 1195.
25. W. Martens, R. L. Frost and J. T. Kloprogge, Journal of Raman Spectroscopy 34 (2003) 90.
26. P. C. Burns, R. C. Ewing and F. C. Hawthorne, Canadian Mineralogist 35 (1997) 1551.
27. F. Hanic, Czechoslovak Journal of Physics 10 (1960) 169.
28. J. Cejka, Reviews in mineralogy 38 (1999).
29. C. Frondel, Am. Mineralogist 36 (1951) 680.
30. K. Walenta, Jahresh. Geol. Landesamtes Baden-Wuerttemberg 6 (1963) 113.
31. R. Vochten and A. Goeminne, Physics and Chemistry of Minerals 11 (1984) 95.
32. J. Cejka, Jr., A. Muck and J. Cejka, Neues Jahrbuch fuer Mineralogie, Monatshefte (1985) 115.
33. V. C. Farmer, *Mineralogical Society Monograph 4: The Infrared Spectra of Minerals*, 1974.

Table 1 X-ray diffraction data analysis of metazeunerite.

sample			00-017-0150 Zeunerite				00-017-0146 Meta-zeunerite			
d [Å]	°2Th.	I [%]	d [A]	°2Th.	I [%]	h k l	d [A]	°2Th.	I [%]	hkl
10.35981	8.5353	100	**10.3**	8.578	100	0 0 2				
8.68233	10.1884	86					**8.86**	9.975	100	0 0 2
			6.81	12.99	30	1 0 1				
6.76185	13.0934	2								
							6.63	13.344	5	1 0 1
							5.57	15.898	80	1 0 2
5.49692	16.1245	1								
5.19651	17.0634	38	**5.2**	17.038	70	0 0 4				
5.05522	17.544	1					**5.1**	17.374	60	1 1 0
4.98093	17.8078	2	**4.98**	17.796	50	1 0 3				
			4.58	19.365	5	1 1 2				
4.35188	20.4076	10					**4.38**	20.258	30	0 0 4
3.71212	23.973	6					**3.73**	23.836	100	1 0 4
3.60126	24.7224	8	**3.59**	24.78	100	2 0 0				
3.55205	25.0705	2					**3.57**	24.921	70	2 0 0
3.46969	25.6756	1								
3.3883	26.3033	3	**3.39**	26.268	50	2 0 2				
3.29142	27.092	1					**3.3**	26.998	80	1 1 4
			3.16	28.218	10	2 1 1	**3.13**	28.494	5	1 0 5
			3.06	29.16	5	2 1 2				
							2.98	29.961	40	2 1 2
2.95158	30.282	1	**2.95**	30.273	30	2 0 4				
			2.91	30.699	5	2 1 3				
			2.86	31.249	10	1 1 6				

							2.77	32.292	10	2 1 3
2.74586	32.5838	2	**2.74**	32.655	30	1 0 7				
2.69008	33.3073	1					**2.69**	33.28	20	1 0 6
2.60112	34.452	1								
2.56742	34.9484	0					**2.57**	34.882	40	2 1 4
			2.53	35.452	40	2 2 0				
2.51501	35.701	0					**2.51**	35.744	40	2 2 0
			2.46	36.496	30	2 2 2				
							2.41	37.281	30	2 2 2
			2.37	37.934	5	3 0 1				
2.31806	38.8507	0	**2.32**	38.784	20	1 1 8				
							2.29	39.312	10	3 0 2
2.2609	39.874	0	**2.26**	39.856	40	3 0 3				
							2.24	40.227	20	3 1 0
2.20136	40.9648	1	**2.21**	40.798	40	3 1 2				
							2.18	41.385	20	0 0 8
2.17761	41.4319	8	**2.18**	41.385	20	2 1 7				
2.1765	41.5619	5								
							2.14	42.195	5	2 1 6
2.08189	43.4313	11								
2.08174	43.5478	5	**2.08**	43.473	60	3 1 4	**2.08**	43.473	30	3 0 4
1.99829	45.3471	1					**1.993**	45.474	40	3 1 4
1.92617	47.1454	1	**1.924**	47.202	60	1 1 10	**1.925**	47.176	10	3 2 2
1.85711	49.0114	0					**1.857**	49.015	5	2 0 8
							1.833	49.699	5	3 0 6
1.79133	50.937	0	**1.794**	50.856	50	4 0 0	**1.796**	50.795	30	2 1 8
							1.776	51.409	30	3 1 6
			1.765	51.753	5	4 0 2				
1.74286	52.4597	1					**1.742**	52.488	5	0 0 10
1.73512	52.7117	1	**1.735**	52.716	5	4 1 1				
			1.708	53.615	10	3 1 8				
			1.69	54.233	10	4 1 3				

			1.661	55.26	5	3 0 9				
1.64176	55.9634	1	**1.64**	56.029	40	1 1 12	**1.643**	55.918	30	3 3 2
1.60295	57.4429	0	**1.602**	57.48	40	4 2 1	**1.602**	57.48	20	3 0 8
			1.584	58.195	10	4 2 2	**1.586**	58.115	20	4 2 0
1.56304	59.0523	0	**1.562**	59.096	20	1 0 13	**1.561**	59.137	60	4 2 2
1.53298	60.329	0	**1.532**	60.372	50	3 1 10				
1.48757	62.3729	1								
1.42421	65.4847	0	**1.427**	65.341	30	1 1 14				
							1.422	65.599	20	1 0 12
1.39459	67.0566	0					**1.395**	67.034	5	1 1 12
			1.378	67.973	40	3 1 12	**1.377**	68.029	30	3 1 10
1.36339	68.8029	1	**1.362**	68.883	30	1 0 15				
1.35969	69.0167	0								
			1.355	69.29	30	5 0 5				
							1.352	69.465	10	4 1 8
							1.325	71.092	10	5 1 4
			1.312	71.906	20	3 3 10				
			1.289	73.396	5	5 2 4				
							1.284	73.729	5	4 2 8
			1.272	74.541	30	5 1 7				
							1.26	75.374	5	5 2 4
			1.245	76.445	40	5 2 6	**1.241**	76.736	5	4 4 2
1.22465	77.9521	0					**1.224**	78.001	10	4 1 10
			1.221	78.23	5	2 0 16				
			1.21	79.079	10	3 3 12	**1.208**	79.236	5	1 1 14
			1.201	79.79	5	5 1 9				
			1.188	80.842	5	6 0 2				
			1.178	81.673	5	4 1 13	**1.175**	81.926	30	2 0 14
			1.165	82.783	40	5 1 10	**1.16**	83.219	20	6 0 3
							1.127	86.235	10	6 1 4
1.1581	83.386	0								
			1.146	84.469	20	4 0 14				

	1.133	85.668	20	4 2 13				
	1.127	86.235	20	3 1 16				
	1.117	87.199	5	6 1 6	**1.113**	87.592	10	6 2 2
					1.101	88.796	5	3 0 14
	1.092	89.724	50	5 1 12	**1.09**	89.934	30	5 2 9
	1.083	90.676	50	4 4 10				
					1.077	91.324	10	1 0 16
					1.065	92.653	10	1 1 16
	1.059	93.335	40	5 3 10				
					1.051	94.264	10	5 2 10
	1.043	95.215	20	3 2 17				
					1.039	95.699	10	6 0 8
	1.036	96.066	40	2 1 19				
					1.029	96.937	20	6 1 8
	1.022	97.827	40	5 1 14				
	1.013	99.002	5	7 1 1	**1.016**	98.606	10	4 3 12
	1.004	100.212	20	5 3 12	**1.006**	99.94	10	5 1 12
	1.001	100.623	30	6 1 11				
	0.998	101.039	30	2 0 20	**0.999**	100.9	20	2 2 16
	0.995	101.46	40	3 0 19				
	0.991	102.027	10	6 4 2				

Table 2 Raman spectroscopic analysis of metazeunerite at elevated temperatures

	20 °C	40 °C	60 °C	80 °C	100 °C	120 °C	Suggested assignments
Band centre/cm^{-1}	890	890	902	902	902	902	UO_2 ν_3
Bandwidth/cm^{-1}	10.0	16.0	18.2	30.9	17.4	19.2	antisymmetric
Relative Intensity/%	6.6	6.83	6.6	9.9	4.3	4.9	stretching
Band centre/cm^{-1}			873	873	867		
Bandwidth/cm^{-1}			26.2	11.0	16.3		
Relative Intensity/%			4.0	0.5	0.87		
Band centre/cm^{-1}					844	842	UO_2 ν_1
Bandwidth/cm^{-1}					19.1	17.0	stretching
Relative Intensity/%					8.8	8.0	modes
Band centre/cm^{-1}	818	822	813	822	813	810	UO_2 ν_1
Bandwidth/cm^{-1}	7.5	9.8	28.6	46.8	36.5	39.0	stretching
Relative Intensity/%	45.8	21.5	32.0	32.0	30.4	37.1	modes
Band centre/cm^{-1}	811	811	801	807	804	805	UO_2 ν_1
Bandwidth/cm^{-1}	10.8	10.8	24.9	24.9	24.1	20.6	stretching
Relative Intensity/%	47.6	70.5	36.8	28.4	24.1	17.9	modes
Band centre/cm^{-1}			775	777	776	778	Water
Bandwidth/cm^{-1}			30.5	34.5	34.3	24.0	librational
Relative Intensity/%			20.2	23.2	26.2	3.4	modes
Band centre/cm^{-1}	463	461					ν_4 bending
Bandwidth/cm^{-1}	19.0	62.7					modes of
Relative Intensity/%	15.6	23.5					AsO_4

Band centre/cm^{-1} Bandwidth/cm^{-1} Relative Intensity/%	446 20.1 26.4	448 17.4 23.2	452 37.3 25.5	452 37.3 25.5	452 37.3 25.5		ν_4 bending modes of AsO_4
Band centre/cm^{-1} Bandwidth/cm^{-1} Relative Intensity/%	396 10.8 0.67	398 18.8 2.0					ν_4 bending modes of AsO_4
Band centre/cm^{-1} Bandwidth/cm^{-1} Relative Intensity/%	380 12.8 1.18		376 49.7 8.0	376 49.7 8.0	376 49.7 8.0		ν_2 bending modes of AsO_4
Band centre/cm^{-1} Bandwidth/cm^{-1} Relative Intensity/%	320 7.1 29.0	318 6.6 22.6	322 16.7 14.8	322 16.7 14.8	322 16.7 14.8		ν_2 bending modes of AsO_4
Band centre/cm^{-1} Bandwidth/cm^{-1} Relative Intensity/%	275 11.0 0.87	274 12.8 2.0	274 43.6 10.1	274 43.6 10.1	274 43.6 10.1		ν_2 bending modes of the $(UO_2)^{2+}$
Band centre/cm^{-1} Bandwidth/cm^{-1} Relative Intensity/%	235 18.9 13.7	241 15.7 1.0					ν_2 bending modes of the $(UO_2)^{2+}$
Band centre/cm^{-1} Bandwidth/cm^{-1} Relative Intensity/%	218 15.0 1.4	214 14.6 10.5	197 28.7 11.3	197 28.7 11.3	197 28.7 11.3		$Cu\text{-}O_{uranyl}$ Stretch (?)
Band centre/cm^{-1} Bandwidth/cm^{-1} Relative Intensity/%		182 10.8 13.6	152 19.6 13.3	152 19.6 13.3	152 19.6 13.3		Lattice modes
Band centre/cm^{-1} Bandwidth/cm^{-1} Relative Intensity/%		139 14.7 1.4	137 11.6 8.1	137 11.6 8.1	137 11.6 8.1		Lattice modes

LIST OF FIGURES

LIST OF TABLES

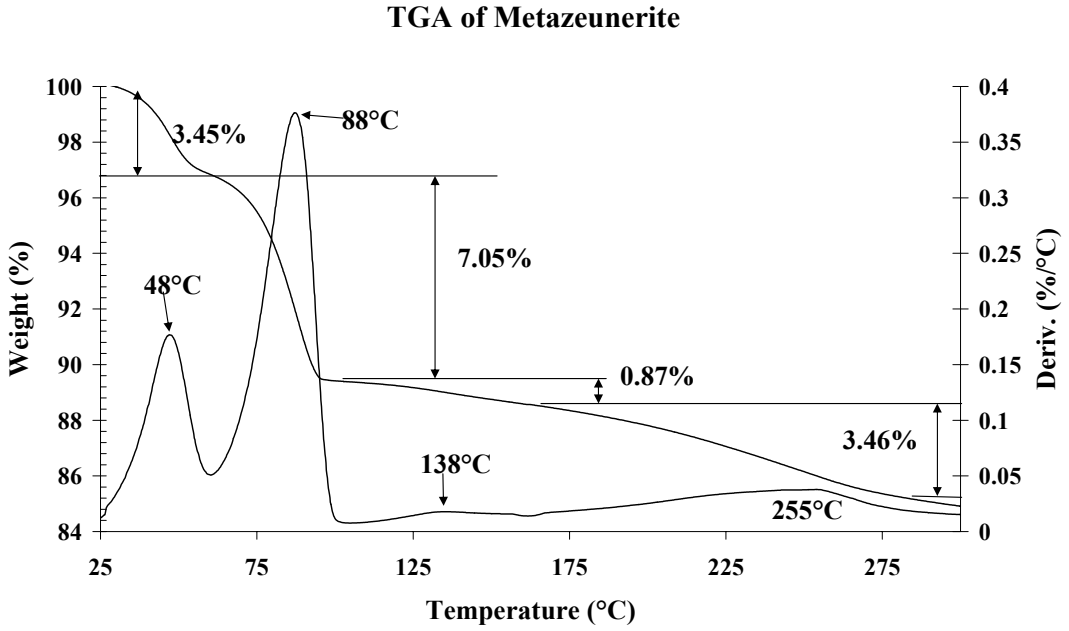

Figure 1a

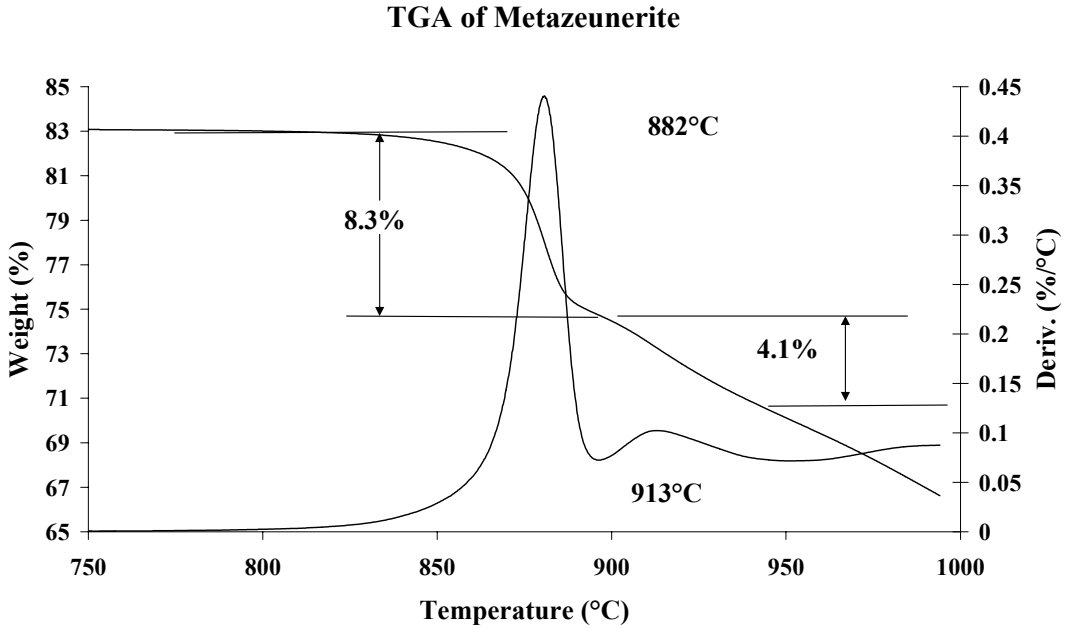

Figure 1b

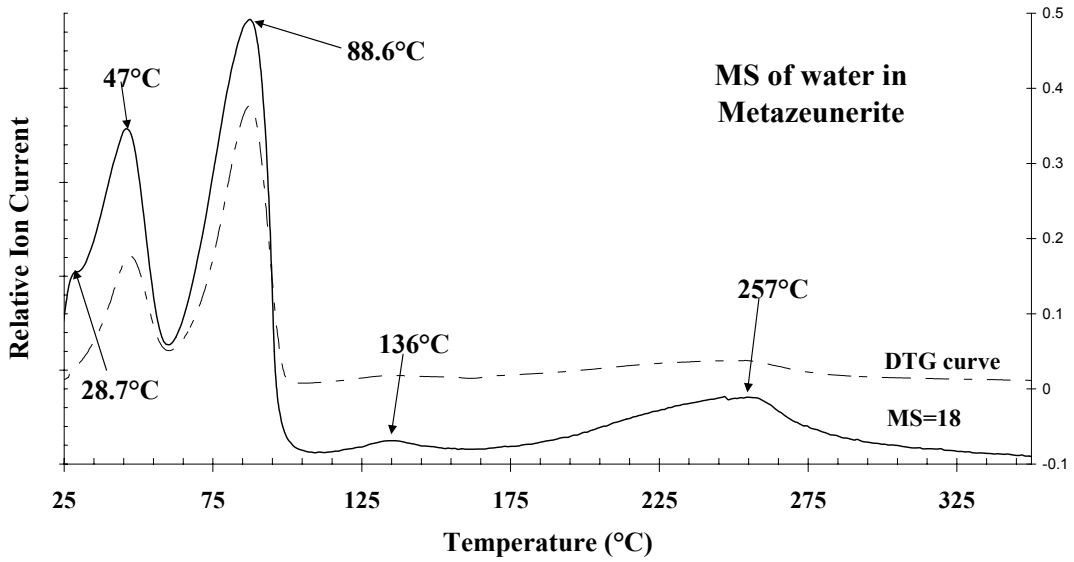
47°C
88.6°C
MS of water in
Metazeunerite
257°C
136°C
28.7°C
DTG curve
MS=18
Relative Ion Current
Temperature (°C)
25
75
125
175
225
275
325
0.5
0.4
0.3
0.2
0.1
0
-0.1

Figure 2

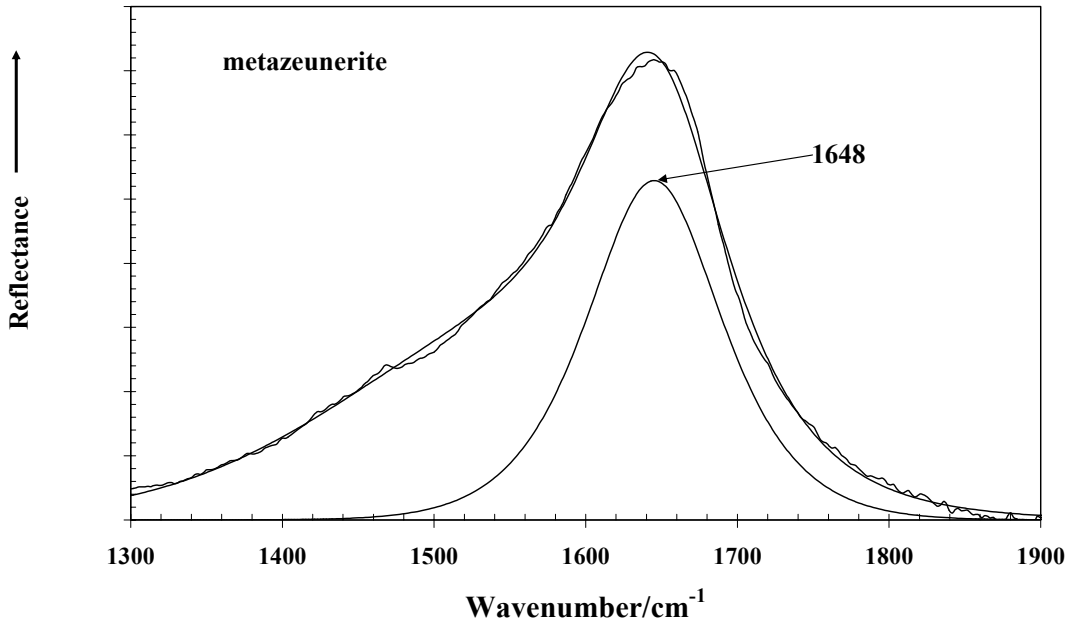
metazeunerite
1648
Reflectance
1300
1400
1500
1600
1700
1800
1900
Wavenumber/cm-1

Figure 3

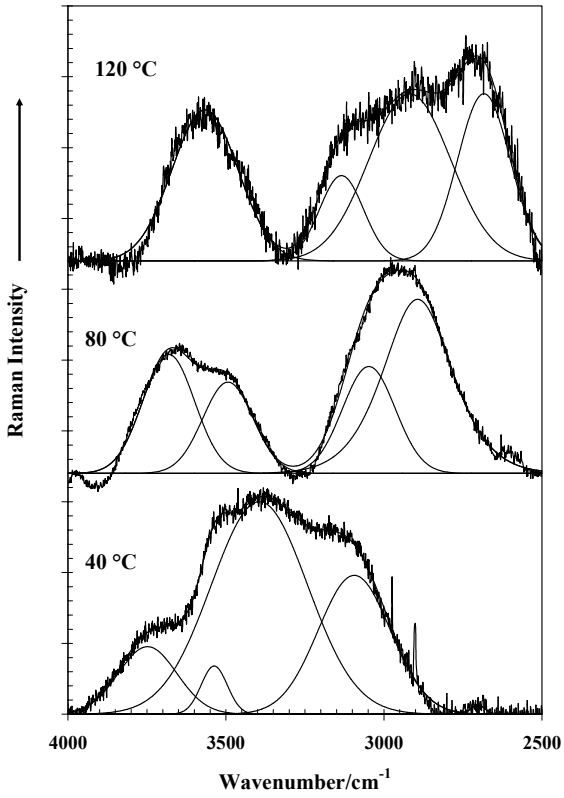
120 °C
80 °C
40 °C
Raman Intensity
4000
3500
3000
2500
Wavenumber/cm-1

Figure 4

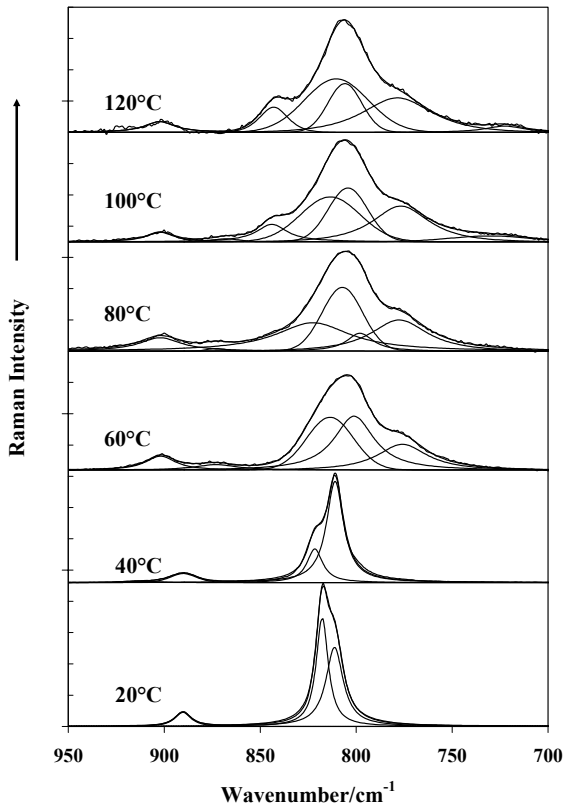
120°C
100°C
80°C
60°C
40°C
20°C
Raman Intensity
950
900
850
800
750
700
Wavenumber/cm-1

Figure 5

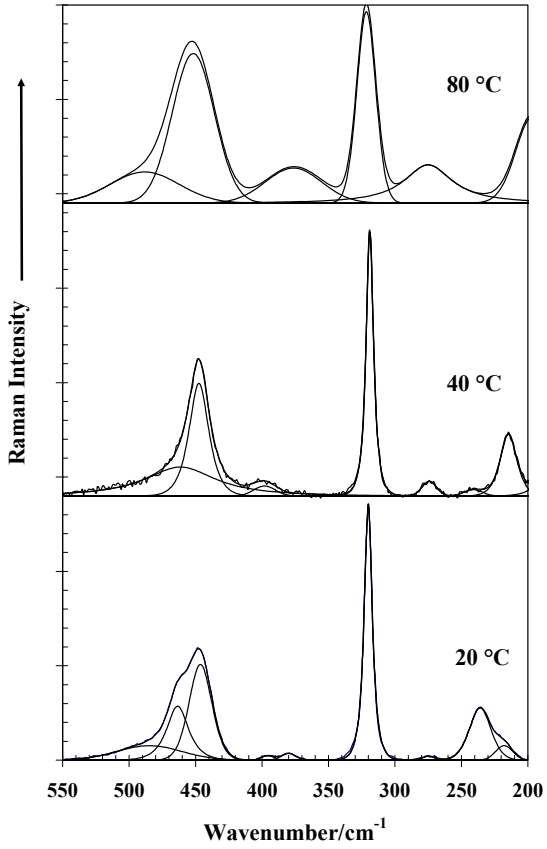
80 °C
40 °C
20 °C
Raman Intensity
550
500
450
400
350
300
250
200
Wavenumber/cm-1

Figure 6